NIH Public Access
Author Manuscript
Magn Reson Med. Author manuscript; available in PMC 2014 November 20.

Published in final edited form as:
Magn Reson Med. 2011 August ; 66(2): 467–475. doi:10.1002/mrm.22854.

*Mo*tion *C*orrection using *C*oil *A*rrays (MOCCA) for Free-Breathing Cardiac Cine MRI

Peng Hu, Ph.D.[1], **Susie Hong, M.D.**[1], **Mehdi H. Moghari, Ph.D.**[1], **Beth Goddu, R.T.**[1], **Lois Goepfert, M.S., R.N.**[1], **Kraig V. Kissinger, M.S., R.T.**[1], **Thomas H. Hauser, M.D.**[1], **Warren J Manning, M.D.**[1,2], and **Reza Nezafat, Ph.D.**[1]

[1]Department of Medicine (Cardiovascular Division), Beth Israel Deaconess Medical Center and Harvard Medical School, Boston, MA, USA

[2]Department of Radiology, Beth Israel Deaconess Medical Center and Harvard Medical School, Boston, MA, USA

Abstract

In this study, we present a motion compensation technique based on coil arrays (MOCCA) and evaluate its application in free-breathing respiratory self-gated cine MRI. MOCCA takes advantages of the fact that motion-induced changes in k-space signal are modulated by individual coil sensitivity profiles. In the proposed implementation of MOCCA self-gating for free-breathing cine MRI, the k-space center line is acquired at the beginning of each k-space segment for each cardiac cycle with 4 repetitions. For each k-space segment, the k-space center line acquired immediately before was used to select one of the 4 acquired repetitions to be included in the final self-gated cine image by calculating the cross-correlation between the k-space center line with a reference line. The proposed method was tested on a cohort of healthy adult subjects for subjective image quality and objective blood-myocardium border sharpness. The method was also tested on a cohort of patients to compare the left and right ventricular volumes and ejection fraction measurements with that of standard breath-hold cine MRI. Our data indicate that the proposed MOCCA method provides significantly improved image quality and sharpness compared to free-breathing cine without respiratory self-gating, and provides similar volume measurements compared with breath-hold cine MRI.

Keywords

motion correction; self-gating; cine MRI; coil arrays

Introduction

Breath-hold cardiac cine MRI is the current clinical gold standard for non-invasive evaluation of cardiac function. In cine MRI, cardiac phase resolved two-dimensional (2D) segmented k-space data are acquired continuously and movies of the beating heart are

Address for correspondence: Reza Nezafat, Ph.D., Beth Israel Deaconess Medical Center, Department of Medicine (Cardiovascular Division), Harvard Medical School, 330 Brookline Avenue, E/SH-455, Boston, MA 02215, Phone: 617-667-1747, rnezafat@bidmc.harvard.edu.

NIH-PA Author Manuscript
NIH-PA Author Manuscript
NIH-PA Author Manuscript

NIH-PA Author Manuscript

NIH-PA Author Manuscript

NIH-PA Author Manuscript

reconstructed by retrospective electrocardiogram (ECG) gating (1). To suppress respiratory motion artifacts, cine MRI is commonly performed during a breath-hold. However, this approach limits a scan to short (<15s) scan times. In addition, many patients are unable to sustain a breath-hold or instead perform a slow exhalation. Alternative methods have been developed for respiratory motion correction that use an abdominal bellow for respiratory gating (2) or use the fat signal to retrospectively correct for respiratory motion (3). The most successful method for high spatial resolution imaging such as coronary artery MRI uses a navigator that monitors the superior-inferior position of the right hemi-diaphragm (4–5). However, navigators are not fully compatible with continuous cine acquisitions because of interruption in steady state signal.

Respiratory self-gating is a promising alternative to breath-holding and navigator gating. In respiratory self-gating, the motion of the heart during free-breathing is estimated from the acquired imaging data. It provides a direct account of the motion of the heart and is not subject to the aforementioned problems. Hardy et al. (6) used cross-correlation of real-time navigator images to estimate the respiratory motion. A similar approach was employed by Sussman et al. (7) using a variable-density spiral acquisition and Larson et al. (8) using a radial acquisition. Radial acquisitions have also been used by others for free-breathing cine MRI due to its inherent over-sampling of k-space center, from which gating signals are commonly derived (9–10). Improved free-breathing cine MRI based on real-time imaging and retrospective image-based registration and re-sorting has also been proposed (11–12). Multiple projection-based methods have been reported for both cine MRI and coronary artery MRI. Uribe et al. (13) used a projection of the heart in the superior-inferior direction to estimate respiratory motion in three-dimensional (3D) cine MRI. Because a projection in the superior-inferior direction was used in this method, the imaging slab has to be in the sagittal orientation and reformatting is required to generate the standard short-axis and long-axis views. Lai et al. developed a respiratory self-gating method for coronary artery MRI using up to six Cartesian projections (14–16) to compensate for 3D respiratory motion. Brau et al. proposed to acquire an additional free induction decay signal in every TR to correct for respiratory motion (17). The efficacy of these methods in cine MRI remains to be investigated.

The extensive availability of multi-coil arrays for parallel imaging offers the opportunity to use the redundant information provided by coil arrays for rigid and non-rigid motion estimation and correction (18–20). In a coil array, each coil has a localized sensitivity profile. Thus, motion of the object relative to the coils causes variations in the received signal. The amount and polarity of these variations may be different among the coils depending on the geometric configuration of each coil. It is therefore possible to take advantages of the differences in the motion-related signal variations between coils to improve motion detection and correction.

In this study, we propose and implement a MOtion Correction technique using Coil Arrays (MOCCA) for free-breathing cine MRI.

NIH-PA Author Manuscript NIH-PA Author Manuscript NIH-PA Author Manuscript

Theory

The k-space data acquired using a surface coil array is modulated by the individual coil sensitivity profiles. Let $v(r)$ be an object and $c_\gamma(r)$ be the coil sensitivity map for the receiver coil γ. The acquired signal is:

$$S^\gamma(k)=\sum_r v(r)c^\gamma(r)W^{r\cdot k} \quad \text{(Eq. 1)}$$

where $W=e^{-j2\pi}$, the Fourier encoding kernel. A motion results in the following k-space signal:

$$\hat{S}^\gamma(k)=\sum_r \tilde{v}(r)c^\gamma(r)W^{r\cdot k}, \quad \text{(Eq. 2)}$$

where $\tilde{v}$ is the object after motion. For non-rigid motion, which is the type of motion studies in this work, the change from $v(r)$ to $\tilde{v}(r)$ reflects the non-rigid deformation of the object. For rigid motion, $\tilde{v}(r)=v(r-\Delta r)$, where Δr is the vector corresponding to the rigid motion. It is then possible to detect and characterize the motion by analyzing the k-space signal change caused by the motion. Furthermore, this motion-induced signal change is modulated by the individual sensitivity profiles of the individual coils and the coils serve as additional "sensors" of the motion. The signal from a coil may change significantly for a small motion in certain direction, but may not change much for motion in another direction. The motion-induced signal change of two coils may even have opposite polarity. Therefore, combination of the signal from multiple coils has the potential to improve motion detection in MRI. In MOCCA, we construct a quantitative measure $Q(\hat{S}^\gamma(k), S^\gamma(k))$ as a representation of the underlying true motion Δr. In reality, it is not feasible or necessary to use the full k-space for this purpose. A subset of the k-space data, such as the k-space center point or the non-phase-encoded k-space center line, is usually sufficient for one to detect the motion. There are many potential definitions for operator Q. For example, it can be defined as the sum of k-space center point signal changes from all the coils: $Q(\hat{S}^\gamma(k), S^\gamma(k))=\Sigma_\gamma \hat{S}^\gamma(0)-S^\gamma(0)$. Alternatively, it can also be defined as the change in the center of mass position of a projection line along the direction of motion, which has been previously used for projection-based self-gating in cardiac MRI (16). It is straightforward to show that the corresponding Q operator for coil channel γ is: $Q(\hat{S}^\gamma(k), S^\gamma(k))=\Sigma_{k\in P} w_k[\hat{S}^\gamma(k)-S^\gamma(k)]$, where P is the set of samples on the non-phase-encoded k-space center line and w_k is a linear factor. It is beyond the scope of this report to investigate the various potential choices of the Q operator and their performances in motion detection. In this work, we sought to evaluate MOCCA with the following real positive scalar Q operator:

$$Q\left(\hat{S}^\gamma(k), S^\gamma(k)\right)=corr\left(|\hat{S}^\gamma(k)|_{k\in P,1\le\gamma\le N}, |S^\gamma(k)|_{k\in P,1\le\gamma\le N}\right) \quad \text{(Eq. 3)}$$

where *corr* calculates cross correlation coefficient (CCC), N is the number of coils, and $|S^\gamma(k)|_{k\in P,1\le\gamma\le N}$ is the vector formed by concatenating the *magnitudes* of non-phase-encoded k-space lines acquired from all of the coils when the object is at a reference position, and $|\hat{S}^\gamma(k)|_{k\in P,1\le\gamma\le N}$ is the vector corresponding to the position after motion. For simplicity, we

NIH-PA Author Manuscript

NIH-PA Author Manuscript

NIH-PA Author Manuscript

herein refer to these vectors as MOCCA echoes and $|\hat{S}^{\gamma}(k)|_{k\in P,1\leq\gamma\leq N}$ as the MOCCA echo reference.

In the basic form of MOCCA imaging, the non-phase-encoded k-space line is sampled at the beginning of each k-space segment. Subsequently these lines (*magnitude* only) from multiple coils are concatenated to form the MOCCA echo. For cardiac cine MRI applications, the duration of data acquisition for each k-space segment is relatively short (<50ms). We assume there is no respiratory motion during that interval and we only account for the respiratory motion between the acquisitions of two successive k-space segments. Hence, in MOCCA, the motion when a k-space segment is acquired is represented by the CCC between the MOCCA echo corresponding to that k-space segment acquisition and the MOCCA echo reference. As demonstrated in the schematic shown in Figure 1, where the object moves away from coil 1 and toward coil 2, the k-space signal amplitude decreases for coil 1 and increases for coil 2. Hence, the concatenation of the non-phase-encoded lines helps in motion detection by taking into account the opposite polarity of the signal changes in coils 1 and 2. The MOCCA echo is then correlated with the MOCCA echo reference. High correlation is expected for small or no motion relative to the reference position, and vice versa. Therefore, the CCC may be used to “gate” respiratory motion in various cardiovascular MRI applications.

Materials and Methods

All imaging was performed on a 1.5 T Achieva MRI system (Philips Healthcare, Best, The Netherlands) using a 32-channel (16 anterior/16 posterior) cardiac array coil (InVivo, Gainesville, FL) or a 5-channel coil (Philips Healthcare, Best, The Netherlands). The 32-channel coil was combined into 16 receiver channels using a combiner. All *in vivo* data were imported into Matlab (MathWorks, Natick, MA) for respiratory self-gating cine MRI reconstruction. Written informed consent was obtained from all the participants of our study and the imaging protocol was approved by our institutional review board.

MOCCA Self-Gated Cine MRI

The respiratory self-gated cine MRI sequence was based on our standard clinical 2D breath-hold 2D steady state free precession (SSFP) cine MRI sequence with retrospective ECG-gating. The non-phase-encoded k-space center line was acquired at the beginning of each k-space segment acquisition for each cardiac phase (Figure 2a). The respiratory self-gated cine MRI sequence was performed on 8 healthy adult subjects (aged 29±16 years, 3 male) in the short-axis, two-chamber, and four-chamber orientations. The sequence was performed during free breathing and was repeatedly acquired 4 times successively. The short-axis image was prescribed at the mid-ventricular level. The sequence parameters included: TR/TE=2.8/1.4 ms, FOV=320 × 320 mm^2, flip angle=60°, resolution=1.8 × 1.8 mm^2, turbo factor=11, acquisition window width=33.6ms. No parallel imaging was prescribed to limit the scope of the differences to gating schemes and motion artifacts rather than the differential impact of parallel imaging.. As a comparison, an additional cine MRI was acquired on each subject using the standard clinical cine MRI sequence with the same sequence parameters except that only a single acquisition was performed during breath-

NIH-PA Author Manuscript

NIH-PA Author Manuscript

NIH-PA Author Manuscript

holding. All the acquired data were subsequently imported into Matlab for retrospective self-gating and reconstruction.

MOCCA Reconstruction

Since each k-space segment for each cardiac phase were acquired four times during free-breathing cine MRI, the basic idea of our MOCCA self-gating algorithm was to choose one of the repetitions for each k-space segment and cardiac phase based on the CCC between their corresponding MOCCA echoes and the MOCCA echo reference (as described below), so that respiratory motion artifacts are suppressed in the reconstructed cine images (Figure 2b). Hence, the MOCCA echoes underwent the follow two steps.

Determination of the MOCCA echo reference—Let N_p, N_s, N_r be the number of cardiac phases, k-space segments and repetitions, respectively. Let $M_{i,j,k}$ be the MOCCA echo corresponding to the i^{th} cardiac phase, j^{th} k-space segment, and k^{th} repetition, where $1 \le i \le N_p, 1 \le j \le N_s, 1 \le k \le N_r$. The MOCCA echo reference was defined as the set of MOCCA echoes acquired during a chosen heart cycle. As the end of expiration is the longest period during a respiratory cycle and is the period when the clinical breath-hold cine MRI is performed, it is desirable to choose MOCCA echoes acquired during this period as the MOCCA echo reference. Let

$$A_{(j,k)} = \frac{\sum_{(l,m,n)} CCC\left(M_{l,(j,k)}, M_{l,(m,n)}\right)}{N_p \times N_s \times N_r} \quad \text{(Eq. 4)}$$

$1 \le l \le N_p$, $1 \le m \le N_s$, $1 \le n \le N_r$ be the average of the CCCs between the MOCCA echoes in the $(j,k)^{th}$ heart beat and the MOCCA echoes with the same cardiac phase acquired in all of the heart beats. The MOCCA echo reference was then chosen as $\tilde{M} = \{M_{i,(j,k)_{ref}}\}_{1 \le i \le N_p}$, where $(j,k)_{ref} = \arg\max_{1 \le (j,k) \le N_s \times N_r} A_{(j,k)}$

MOCCA respiratory self-gating—As shown in Figure 2b, the self-gating reconstruction consisted of the following two steps: 1) The CCCs between every MOCCA echo and the MOCCA echo reference for the same cardiac phase were calculated, i.e. $B_{i,j,k} = corr(\tilde{M}_i, M_{i,j,k})$. 2) Subsequently, for each k-space segment, the imaging data following the MOCCA echo with the highest CCC among all four repetitions was chosen, i.e. $IDX_{i,j} = \arg\max_{1 \le n \le N_r} B_{i,j,n}$, where $IDX_{i,j}$ is the index of the repetition included in the final self-gated image for the i^{th} cardiac phase and j^{th} k-space segment.

In addition to the MOCCA self-gated cine reconstruction, the first acquisition of the free-breathing cine MRI data set was used to reconstruct a free-breathing cine image without self-gating. For validation, the clinical breath-hold cine MRI data were also retrospectively reconstructed in Matlab.

Cardiac Function Evaluation

The proposed respiratory self-gating cine MRI sequence was further compared with the standard clinical breath-hold cine MRI with short-axis stacks in terms of cardiac volume

NIH-PA Author Manuscript

NIH-PA Author Manuscript

NIH-PA Author Manuscript

measurements. On 14 patients who were referred to cardiac MR in our center (9 atrial fibrillation patients referred for evaluation of pulmonary vein and left atrium anatomy and 5 congestive heart failure patients referred for evaluation of cardiac function and viability), the proposed sequence was performed within the same imaging session as the clinical scan. The imaging parameters and volume coverage of the proposed free-breathing cine MRI was the same as the healthy subject study. 10–12 short-axis slices were prescribed to cover both ventricles.

Data Analysis

Sharpness—The sharpness of the blood-myocardium border sharpness was evaluated on the images acquired on the healthy subjects using a method similar to that used by Larson et al. (8). For each cine image, the signal intensity profile of a straight line crossing the blood-myocardium border in mid-diastolic cine images was extracted and the sharpness score was calculated as $\frac{1}{D}$, where D is the distance (in mm) between the two points along the profile with 20% and 80% signal intensity, respectively. For short axis and four-chamber cine images, the profile was drawn across the ventricular septum and the sharpness scores on both sides of the septum were averaged. For two-chamber images, the line was drawn on the anterior LV wall. The profiles lines drawn for the three reconstructions methods were at the same location to maintain consistency.

Subjective Image Grading—The quality of the cine images from the breath-held, free-breathing with and without MOCCA self-gating were graded by 2 expert evaluators (with 10 years and 5 years of experience, respectively) in a consensus reading blinded to the subject and sequence information using a 4 point scale (1=poor, 2=fair, 3=good, and 4=very good). The reconstructed cine images were saved as movie files and the three cine movies for each data set were presented to the evaluators on a computer workstation side by side, with the order in which these movies were presented being randomized.

Cardiac Volume Measurements—The free-breathing cine data from the patients were exported to Matlab where MOCCA self-gating was performed. After reconstruction, the self-gated images were pushed back into the ViewForum workstation (Philips Healthcare, Best, the Netherlands), where the LV end-diastolic volume (LVEDV), LV end-systolic volume (LVESV), RV end-diastolic volume (RVEDV), RV end-systolic volume (RVESV), left ventricular ejection fraction (LVEF), and right ventricular ejection fraction (RVEF) were measured by an experienced cardiologist using commercially available software included on the ViewForum workstation. The volume measurements were performed again on the standard breath-hold cine images.

Statistical Analysis

All statistical tests were performed using SAS (v9.1, SAS Institute Inc., Cary, NC). The sharpness scores were analyzed using a t-test. The subjective grading scores from all three methods were compared using a linear mixed-effects model with compound symmetry variance-covariance structure for the error matrix and linear contrasts (21). A Bonferroni correction was applied for multiple comparisons. For the patient data, the level of agreement

NIH-PA Author Manuscript

NIH-PA Author Manuscript

NIH-PA Author Manuscript

between the LV and RV volume and ejection fraction measurements from the two cine data sets were compared using Bland-Altman analysis. The range of agreement was defined as mean bias ± 1.96 standard deviation. A two-sided p-value of <0.05 was used to determine statistical significance.

Results

Figures 3–5 show example cine images in short-axis, 2-chamber and 4-chamber long-axis views acquired on three healthy subjects, respectively. There were obvious respiratory motion-related blurring and artifacts in the free-breathing images without motion gating. MOCCA self-gating successfully removed these artifacts, resulting image quality was comparable to that acquired with standard breath-hold cine MRI.

The blood-myocardium border sharpness scores are summarized in Table 1. The sharpness scores for MOCCA self-gated and breath-hold cine images were both significantly higher than the free-breathing reconstruction without motion gating in all three orientations (P=0.004, 0.01 and <0.001 for short-axis, 2 chamber and 4 chamber views, respectively). The sharpness scores for MOCCA self-gated images were similar to that of the standard breath-hold cine MRI (P=NS for all three orientations).

Table 2 shows the subjective image scores. The scores of standard breath-held cine MRI and MOCCA self-gated cine MRI were both significantly better than free-breathing without motion gating (P<0.001 after Bonferroni correction). The scores of breath-hold cine MRI was similar to MOCCA self-gated cine MRI (P=NS). The effect of cine image orientation on the scores were not significant (P=NS).

Figure 6 shows typical multi-slice short-axis cine images acquired for a patient during breath-hold (top) and free-breathing MOCCA self-gating (bottom). Across all of the slices covering the LV and RV, the proposed self-gating method provided comparable image quality to breath-hold that allowed accurate volume and ejection fraction measurements shown in Figure 7. LV and RV volumes and ejection fraction measurements based on the proposed self-gated cine MRI method were similar to breath-hold cine MRI. The Bland-Altman analysis indicated that the 95% limits of agreement between the measurements based on the standard breath-hold cine MRI and the proposed self-gated cine MRI method were −7.8±15.0 ml for LVEDV, −2.7±8.7 ml for LVESV, −6.1±17.2 ml for RVEDV, −3.5±11.9 ml for RVESV, 0.4%±4.4% for LVEF, and 0.4%±5.4% for RVEF. The mean bias and 95% limits of these volume and ejection fraction data were considered acceptable for application of this technique.

Discussions

In this study, we introduce MOCCA as a respiratory motion compensation and self-gating technique that takes advantages of the additional information offered by multi-coil arrays. We evaluated the MOCCA implementation that concatenates the non-phase-encoded k-space center lines as a representation of the underlying motion of interest. We tested the MOCCA technique on respiratory self-gated free-breathing cine MRI. The proposed technique eliminates the need for breath-holding, which may be problematic for certain

NIH-PA Author Manuscript

NIH-PA Author Manuscript

NIH-PA Author Manuscript

patients, while providing similar blood-myocardium border sharpness and cardiac function measurements compared to gold-standard breath-hold cine MRI.

The proposed technique is a retrospective self-gating method based on 4 repetitions of cine data. As the goal of our study was to demonstrate the feasibility of the proposed technique, the number of repetitions required may not be optimal and should be further studied. In addition, compared to a prospective approach, retrospective self-gating carries the risk of acquiring all 4 repetitions outside the desired gating position. Therefore, it would be desirable to implement the self-gating method prospectively to better adapt to the breathing pattern of individual subjects.

The proposed technique is different from existing respiratory self-gated cine MRI methods in both pulse sequences and self-gating algorithm. Compared to existing respiratory self-gating methods for cine MRI using radial trajectory, the proposed method is based on Cartesian sampling, which is clinically more widely used. A recent respiratory self-gating method for cine MRI (8) requires a series of low-resolution navigator images, which are not required in the MOCCA self-gating. Uribe et al. (13) proposed a respiratory self-gated whole-heart cine MRI method using the conventional projection-based approach, where the imaging slab is required to be prescribed in the sagittal orientation to enable acquisition of a projection signal in the superior-inferior direction. As a result, reformatting is required to obtain cine images in the traditional short-axis or long-axis orientation. In our method, the MOCCA echo may be acquired in arbitrary double-oblique direction. This enables 2D cine MRI in the standard short axis or long axis views, as demonstrated in our results. This was possible because MOCCA relies on the signal changes caused by the relative motion between the object and the two-dimensional coil sensitivity profiles, instead of the k-space phase ramp in the direction of motion. Therefore, the one-dimensional MOCCA echo has the intrinsic capability to detect motion in directions other than the direction of the k-space center line.

Our studies focused on investigating the efficacy of MOCCA in cine MRI. It remains to be assessed whether MOCCA can be used in other high resolution cardiac imaging application, such as perfusion and coronary artery MRI. In coronary MRI, the motion of the coronary arteries is commonly assumed to be 60% of the superior-inferior motion of the right hemidiaphragm (4), where the navigator echo is commonly placed. However, this ratio has been shown to be subject specific (22). MOCCA, like other self-gating methods (15), may be advantageous because it directly monitors the motion of the heart. Furthermore, the traditional navigator echo is commonly placed before and/or after the imaging shot with a time gap of 30–40ms. Any motion during the time gap is not accounted for in the motion compensation. This is not problematic in MOCCA self-gating and other self-gating methods in general since the MOCCA echoes can be easily placed at the beginning, end or in the middle of the imaging shot, which eliminates this time gap. Additionally, the MOCCA echo signal can be potentially integrated into the imaging data set as an extra k-space center signal to improve image reconstruction. Therefore, MOCCA may be a valuable addition to traditional navigators in further improving respiratory motion compensation in these applications.

NIH-PA Author Manuscript

NIH-PA Author Manuscript

NIH-PA Author Manuscript

It is the purpose of our study to demonstrate the feasibility of the MOCCA method. Further improvements in the design and implementation of MOCCA based on specific applications are likely. To improve MOCCA self-gating, it is necessary to further study and optimize the choice of coils included in the MOCCA echo. In our study, we included all available coils, which might not be optimal as inclusion of coils with low signals or spatially invariant coil sensitivity in the direction of motion might negatively affect the ability of MOCCA to detect motion as signal for these coils mainly contribute noise. These coils should be excluded in the MOCCA algorithm or they should be less weighted in the formation of MOCCA echo. It may be possible to determine the weighting of an individual coil by studying its coil sensitivity profile. In this work, both the anterior and posterior coils are used. During free breathing, the anterior coils will move with the chest wall. As a result, the assumption in Eq. 2 that the coil sensitivity profile $c^{\gamma}(r)$ does not move is no longer valid. Fortunately, for the self-gating method presented in this work, this should not affect the periodicity of the self-gating signal or the self-gating results. However, this point should be considered in future potential applications of MOCCA. In our MOCCA self-gating algorithm, only the *magnitude* of the MOCCA echoes was used. The modulation of the k-space signal by the coil map results in a change in k-space signal *magnitude* for a moving object, in addition to the k-space phase ramp predicted by Fourier theory. A potential problem with using k-space phase only is the 2π phase wrapping resulting from larger motions. Nevertheless, the phase information may be incorporated into the current formulation of MOCCA to achieve benefits, as this information is readily available without penalty in imaging sequence. Inclusion of k-space phase in the formation of MOCCA echoes should also reduce the likelihood of the rare coincidence where two different motion states have the same CCC with the MOCCA echo reference. Further study is required to investigate whether and how to include the k-space phase information in the algorithm to further improve the accuracy of self-gating.

The extensive use of multi-coil arrays to accelerate image acquisition using parallel imaging (23) offers the opportunity to use the redundant information provided by coil arrays for motion estimation and correction (18–20). The recently proposed respiratory self-gating methods used either a single coil from a coil array or a linear combination of multiple coil signals. The concept of forming a MOCCA echo by concatenating the k-space center lines into a vector may be readily integrated to existing methods such as that proposed by Uribe et al. (13) and potentially achieve further improvements on those methods.

Our study has limitations. Although our algorithm for generating MOCCA echo reference tends to select a MOCCA echo acquired at end-expiration, we did not have data to support that. Therefore, the respiratory position of the MOCCA self-gated and breath-hold images might not be at exactly the same respiratory position. Therefore, further study is needed to investigate and optimize the method for choosing the MOCCA echo reference.

In conclusion, we demonstrated the feasibility and benefits of MOCCA in free-breathing respiratory self-gating cine MRI. Further study is required for better understanding MOCCA and its ability to resolve motion in MRI.

NIH-PA Author Manuscript

NIH-PA Author Manuscript

NIH-PA Author Manuscript

Acknowledgments

The authors acknowledge funding support from the National Institutes of Health (5R01EB008743-02), American Heart Association (AHA SDG-0730339N and AHA 10SDG4200076) and Harvard Clinical and Translational Science Center, National Center for Research Resources (UL1 RR025758-01).

References

1. Nijm GM, Sahakian AV, Swiryn S, Carr JC, Sheehan JJ, Larson AC. Comparison of self-gated cine MRI retrospective cardiac synchronization algorithms. J Magn Reson Imaging. 2008; 28(3):767–772. [PubMed: 18777546]
2. Yuan Q, Axel L, Hernandez EH, Dougherty L, Pilla JJ, Scott CH, Ferrari VA, Blom AS. Cardiac-respiratory gating method for magnetic resonance imaging of the heart. Magn Reson Med. 2000; 43(2):314–318. [PubMed: 10680698]
3. Keegan J, Gatehouse PD, Yang GZ, Firmin DN. Non-model-based correction of respiratory motion using beat-to-beat 3D spiral fat-selective imaging. J Magn Reson Imaging. 2007; 26(3):624–629. [PubMed: 17729350]
4. Wang Y, Riederer SJ, Ehman RL. Respiratory motion of the heart: kinematics and the implications for the spatial resolution in coronary imaging. Magn Reson Med. 1995; 33(5):713–719. [PubMed: 7596276]
5. Wang Y, Ehman RL. Retrospective adaptive motion correction for navigator-gated 3D coronary MR angiography. J Magn Reson Imaging. 2000; 11(2):208–214. [PubMed: 10713956]
6. Hardy CJ, Saranathan M, Zhu Y, Darrow RD. Coronary angiography by real-time MRI with adaptive averaging. Magn Reson Med. 2000; 44(6):940–946. [PubMed: 11108632]
7. Sussman MS, Stainsby JA, Robert N, Merchant N, Wright GA, Bock JC. Variable-density adaptive imaging for high-resolution coronary artery MRI. Magn Reson Med. 2002; 48(5):753–764. [PubMed: 12417989]
8. Larson AC, Kellman P, Arai A, Hirsch GA, McVeigh E, Li D, Simonetti OP. Preliminary investigation of respiratory self-gating for free-breathing segmented cine MRI. Magn Reson Med. 2005; 53(1):159–168. [PubMed: 15690515]
9. Leung AO, Paterson I, Thompson RB. Free-breathing cine MRI. Magn Reson Med. 2008; 60(3): 709–717. [PubMed: 18727100]
10. Liu J, Spincemaille P, Codella NC, Nguyen TD, Prince MR, Wang Y. Respiratory and cardiac self-gated free-breathing cardiac CINE imaging with multiecho 3D hybrid radial SSFP acquisition. Magn Reson Med. 2010; 63(5):1230–1237. [PubMed: 20432294]
11. Kellman P, Chefd'hotel C, Lorenz CH, Mancini C, Arai AE, McVeigh ER. Fully automatic, retrospective enhancement of real-time acquired cardiac cine MR images using image-based navigators and respiratory motion-corrected averaging. Magn Reson Med. 2008; 59(4):771–778. [PubMed: 18302227]
12. Kellman P, Chefd'hotel C, Lorenz CH, Mancini C, Arai AE, McVeigh ER. High spatial and temporal resolution cardiac cine MRI from retrospective reconstruction of data acquired in real time using motion correction and resorting. Magn Reson Med. 2009; 62(6):1557–1564. [PubMed: 19780155]
13. Uribe S, Muthurangu V, Boubertakh R, Schaeffter T, Razavi R, Hill DL, Hansen MS. Whole-heart cine MRI using real-time respiratory self-gating. Magn Reson Med. 2007; 57(3):606–613. [PubMed: 17326164]
14. Lai P, Larson AC, Bi X, Jerecic R, Li D. A dual-projection respiratory self-gating technique for whole-heart coronary MRA. J Magn Reson Imaging. 2008; 28(3):612–620. [PubMed: 18777542]
15. Lai P, Larson AC, Park J, Carr JC, Li D. Respiratory self-gated four-dimensional coronary MR angiography: a feasibility study. Magn Reson Med. 2008; 59(6):1378–1385. [PubMed: 18506786]
16. Lai P, Bi X, Jerecic R, Li D. A respiratory self-gating technique with 3D-translation compensation for free-breathing whole-heart coronary MRA. Magn Reson Med. 2009; 62(3):731–738. [PubMed: 19526514]

NIH-PA Author Manuscript

NIH-PA Author Manuscript

NIH-PA Author Manuscript

17. Brau AC, Brittain JH. Generalized self-navigated motion detection technique: Preliminary investigation in abdominal imaging. Magn Reson Med. 2006; 55(2):263–270. [PubMed: 16408272]

18. Bydder M, Atkinson D, Larkman DJ, Hill DL, Hajnal JV. SMASH navigators. Magn Reson Med. 2003; 49(3):493–500. [PubMed: 12594752]

19. Bammer R, Aksoy M, Liu C. Augmented generalized SENSE reconstruction to correct for rigid body motion. Magn Reson Med. 2007; 57(1):90–102. [PubMed: 17191225]

20. Atkinson D, Larkman DJ, Batchelor PG, Hill DL, Hajnal JV. Coil-based artifact reduction. Magn Reson Med. 2004; 52(4):825–830. [PubMed: 15389945]

21. Laird MN, Ware HJ. Random-effects models for longitudinal data. Biometrics. 1982; 38:963–974. [PubMed: 7168798]

22. Danias PG, Stuber M, Botnar RM, Kissinger KV, Edelman RR, Manning WJ. Relationship between motion of coronary arteries and diaphragm during free breathing: lessons from real-time MR imaging. AJR Am J Roentgenol. 1999; 172(4):1061–1065. [PubMed: 10587147]

23. Pruessmann KP, Weiger M, Scheidegger MB, Boesiger P. SENSE: sensitivity encoding for fast MRI. Magn Reson Med. 1999; 42(5):952–962. [PubMed: 10542355]

NIH-PA Author Manuscript

NIH-PA Author Manuscript

NIH-PA Author Manuscript

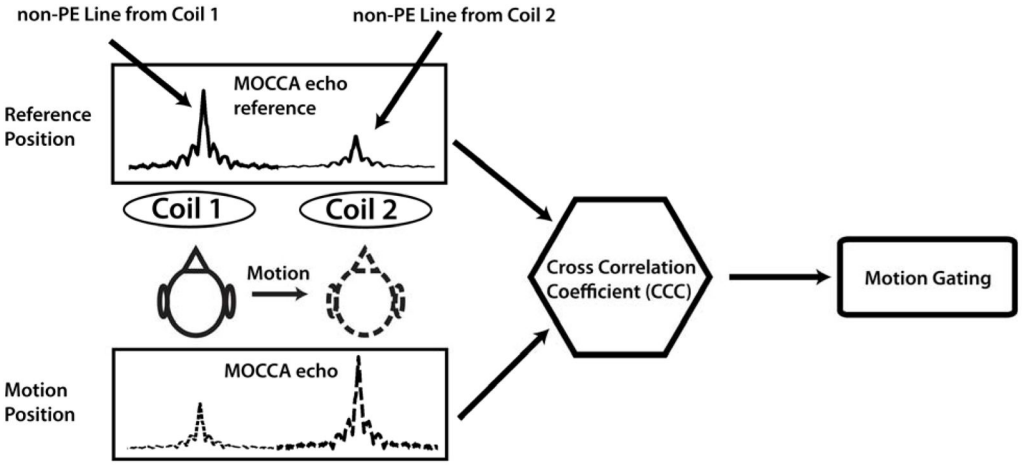

Figure 1.

A schematic of MOCCA. Motion causes variations in the non-phase-encoded (non-PE) k-space center line signal, subject to modulation by the individual coil sensitivity profiles. In this example scenario, the coil 1 signal decreases while coil 2 signal increases after motion. The concatenated non-PE lines (MOCCA echo) take advantage of the additional information provided by multiple coils, which serve as additional “motion sensors”. The cross correlation coefficient (CCC) between the MOCCA echoes acquired before (reference position) and after motion represents the underlying true motion.

NIH-PA Author Manuscript

NIH-PA Author Manuscript

NIH-PA Author Manuscript

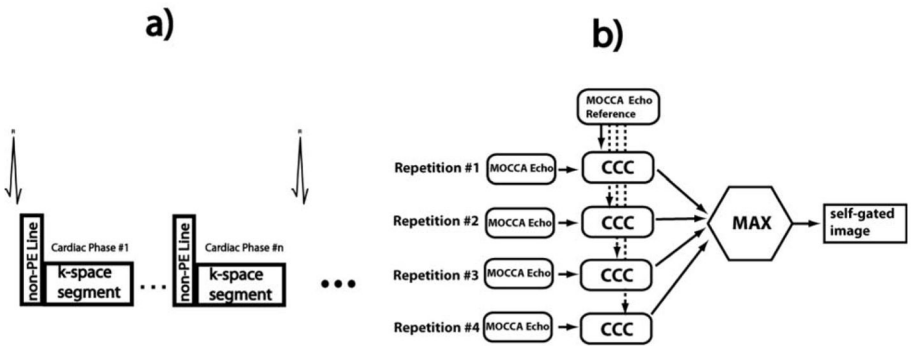

Figure 2.

a) Free-breathing respiratory self-gated cine MRI sequence. The non-PE k-space center line is acquired before each imaging segment for every cardiac phase. b) MOCCA respiratory self-gating algorithm. Each k-space segment for each cardiac phase was acquired four times. Each corresponding MOCCA echo was correlated with a MOCCA echo reference. The imaging segment corresponding to the MOCCA echo with maximum cross correlation coefficient (CCC) is included in the final self-gated cine image.

NIH-PA Author Manuscript

NIH-PA Author Manuscript

NIH-PA Author Manuscript

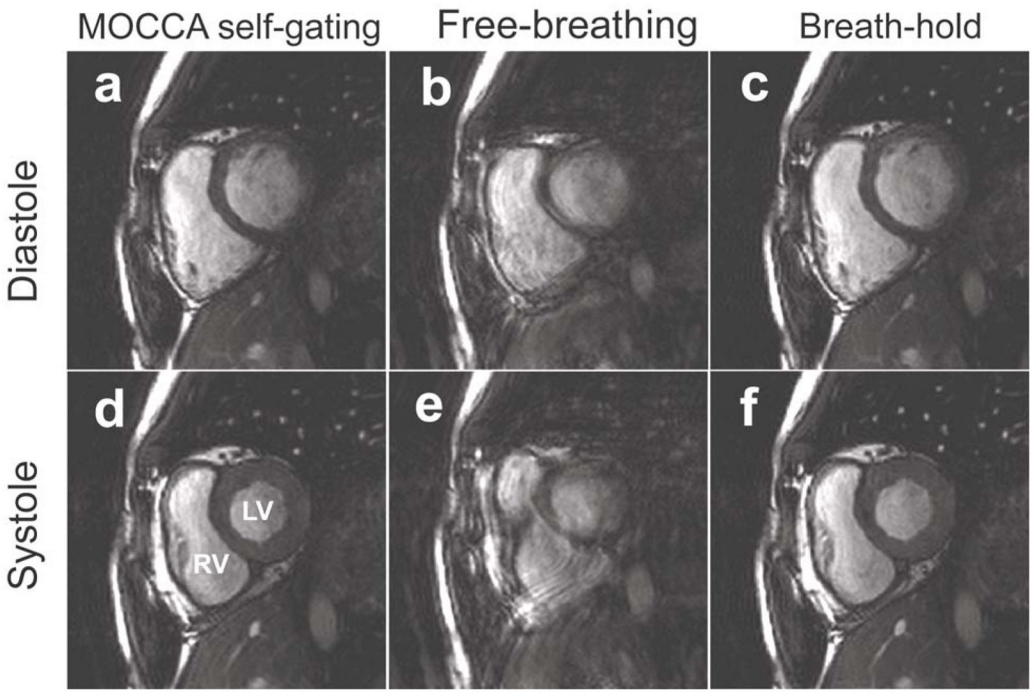

Figure 3.

Example short-axis cine images of diastole (top row) and systole (bottom row) obtained from MOCCA self-gating (a,d), free-breathing without motion correction (b,e) and conventional breath-hold cine (c,f). Obvious blurring and artifacts due to respiratory motion are observed in free-breathing cine MRI without motion gating. These artifacts are eliminated in MOCCA self-gated images, resulting in comparable image quality to conventional breath-hold cine MRI. LV: left ventricle. RV: right ventricle

NIH-PA Author Manuscript

NIH-PA Author Manuscript

NIH-PA Author Manuscript

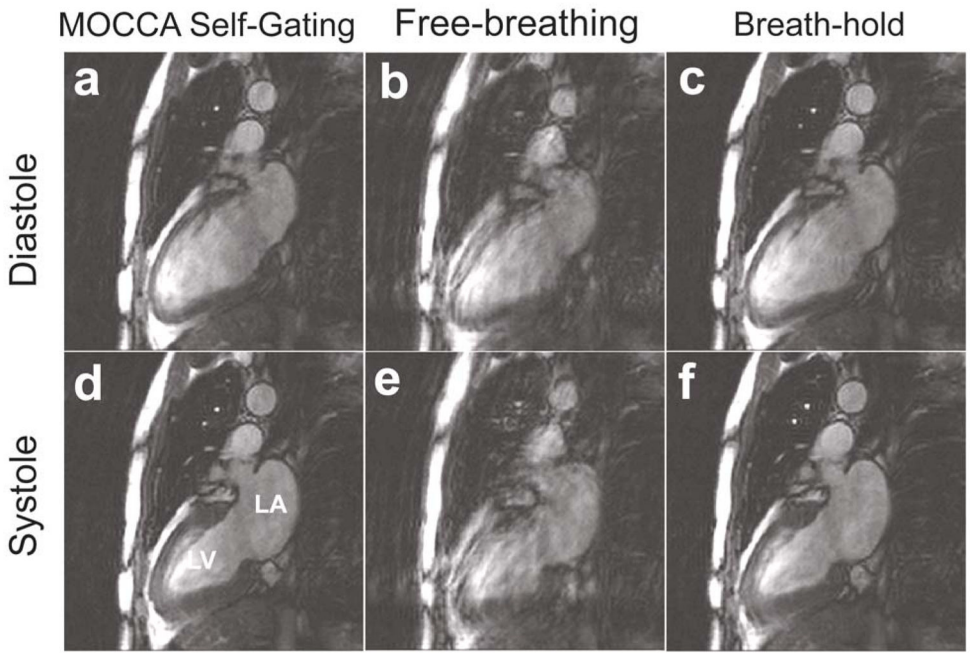

Figure 4.

Example cine images in 2-chamber view of diastole (top row) and systole (bottom row) obtained from MOCCA self-gating (a,d), free-breathing without motion gating (b,e) and conventional breath-hold cine (c,f). LA: left atrium

NIH-PA Author Manuscript

NIH-PA Author Manuscript

NIH-PA Author Manuscript

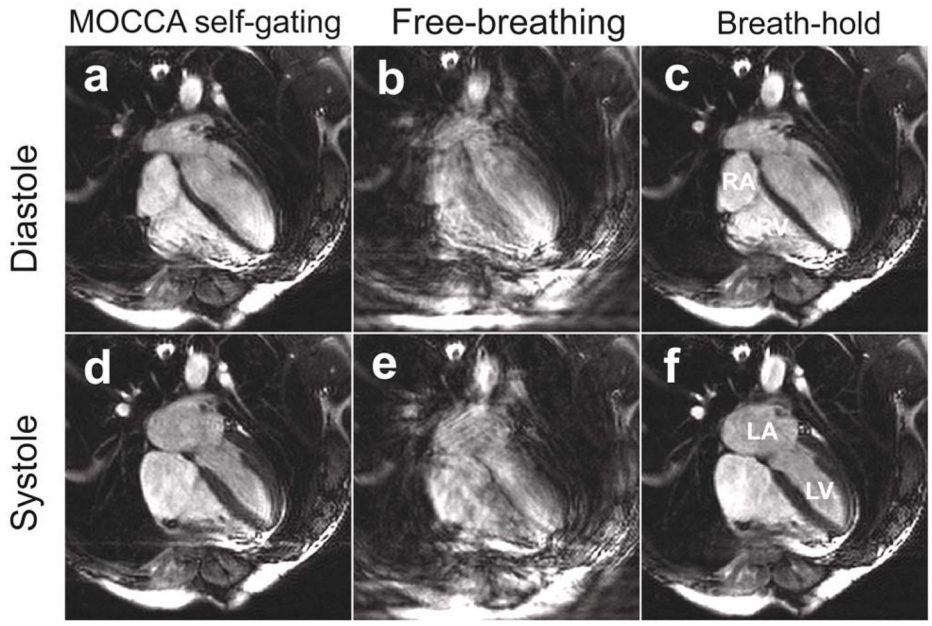

Figure 5.

Example cine images in 4-chamber view of diastole (top row) and systole (bottom row) obtained from MOCCA self-gating (a,d), free-breathing without motion gating (b,e) and conventional breath-hold cine (c,f). Significant image artifacts due to respiratory motion can be observed in free-breathing cine that are eliminated in MOCCA.

NIH-PA Author Manuscript

NIH-PA Author Manuscript

NIH-PA Author Manuscript

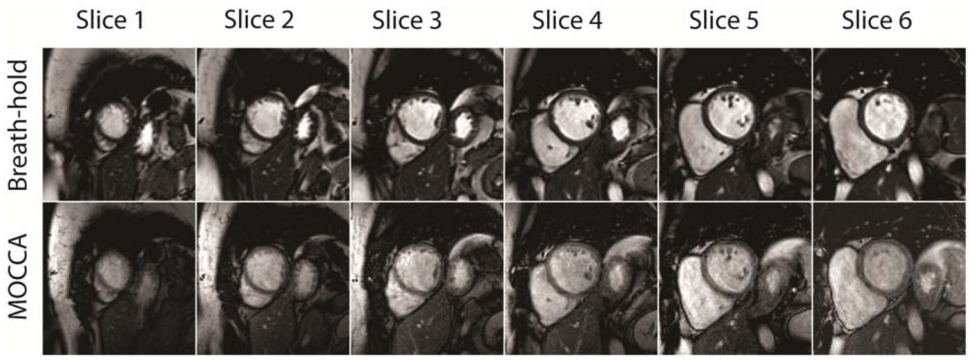

Figure 6.

Example of typical short-axis cine images acquired during (top row) breath-hold and (bottom row) free-breathing with MOCCA self-gating.

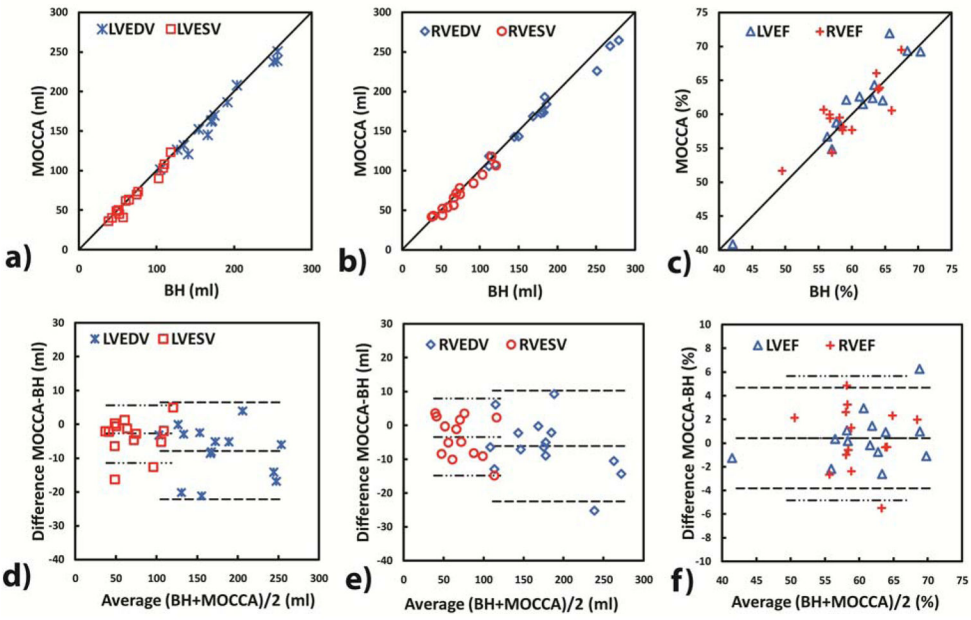

Figure 7.

Comparison of left ventricular (LV) and right ventricular (RV) volumes and ejection fraction measurements from free-breathing MOCCA self-gated and standard breath-hold cine MRI acquisitions based on (a,b,c) plot of identify and (d,e,f) Bland-Altman plot for (a,d) LV volumes, (b,e) RV volumes and (c,f) LV/RV ejection fraction measurements. LVEDV: LV end-diastolic volume, LVESV: LV end-systolic volume. RVEDV: RV end-diastolic volume. RVESV: RV end-systolic volume. LVEF: LV ejection fraction. RVEF: RV ejection fraction. BH: breath-hold.

NIH-PA Author Manuscript NIH-PA Author Manuscript NIH-PA Author Manuscript

NIH-PA Author Manuscript

NIH-PA Author Manuscript

NIH-PA Author Manuscript

Table 1

Quantitative blood-myocardium border sharpness of cine MRI using three methods (free breathing, breath-hold, and MOCCA self-gating). [Higher is better]

	SA	2CH	4CH
MOCCA self-gating	0.50±0.19*#	0.43±0.16*#	0.46±0.15*#
Free-breathing (No Gating)	0.28±0.15	0.28±0.14	0.24±0.12
Breath-hold	0.58±0.26*	0.62±0.22*	0.48±0.13*

*$P<0.05$ when compared with free-breathing.

#P =NS when compared with breath-hold.

SA=short axis; CH=chamber.

NIH-PA Author Manuscript
NIH-PA Author Manuscript
NIH-PA Author Manuscript

Table 2

Subjective image scores on the heart and non-cardiac structures of cine MRI using three methods (free breathing, breath-hold, and MOCCA self-gating). [Higher is better.]

	Heart			Non-Cardiac		
	SA	**2CH**	**4CH**	**SA**	**2CH**	**4CH**
MOCCA Self-gating	3.4±0.7*#	3.5±0.7*#	3.5±0.5*#	3.3±0.9*#	3.6±0.7*#	3.6±0.8*#
Free-breathing (No Gating)	2.0±1.0	2.4±1.1	2.5±0.9	2.0±1.1	3.2±0.7	3.3±1.0
Breath-hold	4.0±0.0*	3.8±0.4*	4.0±0.0*	4.0±0.0*	4.0±0.0*	4.0±0.0*

*P<0.05 when compared with free-breathing.

#P =NS when compared with breath-hold.

Magn Reson Med. Author manuscript; available in PMC 2014 November 20.